THE JOURNAL OF BIOLOGICAL CHEMISTRY VOL. 284, NO. 47, pp. 32725–32734, November 20, 2009

Role of Spike Protein Endodomains in Regulating Coronavirus Entry*

Received for publication, July 10, 2009, and in revised form, September 29, 2009 Published, JBC Papers in Press, September 30, 2009, DOI 10.1074/jbc.M109.043547

Ana Shulla and Tom Gallagher[1]

From the Department of Microbiology and Immunology, Loyola University Medical Center, Maywood, Illinois 60153

Enveloped viruses enter cells by viral glycoprotein-mediated binding to host cells and subsequent fusion of virus and host cell membranes. For the coronaviruses, viral spike (S) proteins execute these cell entry functions. The S proteins are set apart from other viral and cellular membrane fusion proteins by their extensively palmitoylated membrane-associated tails. Palmitate adducts are generally required for protein-mediated fusions, but their precise roles in the process are unclear. To obtain additional insights into the S-mediated membrane fusion process, we focused on these acylated carboxyl-terminal intravirion tails. Substituting alanines for the cysteines that are subject to palmitoylation had effects on both S incorporation into virions and S-mediated membrane fusions. In specifically dissecting the effects of endodomain mutations on the fusion process, we used antiviral heptad repeat peptides that bind only to folding intermediates in the S-mediated fusion process and found that mutants lacking three palmitoylated cysteines remained in transitional folding states nearly 10 times longer than native S proteins. This slower refolding was also reflected in the paucity of postfusion six-helix bundle configurations among the mutant S proteins. Viruses with fewer palmitoylated S protein cysteines entered cells slowly and had reduced specific infectivities. These findings indicate that lipid adducts anchoring S proteins into virus membranes are necessary for the rapid, productive S protein refolding events that culminate in membrane fusions. These studies reveal a previously unappreciated role for covalently attached lipids on the endodomains of viral proteins eliciting membrane fusion reactions.

Biological membranes are configured in large part by protein-mediated fission and fusion reactions. Enveloped viruses can reveal the principles of these processes because their assembly and budding from infected cells requires membrane fissions, and their entry into susceptible cells depends on membrane fusions. Glycoproteins extending from virion surfaces mediate the fusion process. These specialized integral membrane proteins are in metastable high energy configurations on virus surfaces, and they drive coalescence of opposing virus and cell membranes by undergoing a series of energy-releasing unfolding and refolding events (1). The structural rearrangements are triggered by virus binding to cellular receptors (2) and by the acidic, proteolytic environments encountered after viruses are endocytosed (3–5). These reactions begin with an unfolding process that reveals hydrophobic fusion peptides (FPs)[2] that dagger into cellular membranes. This is then followed by a refolding process that, in analogy to a closing hairpin, brings FPs and associated cellular membranes toward the virion membranes, driving formation of a lipid stalk connecting the opposing outer membrane leaflets (6) and culminating in complete cell-virion membrane coalescence (7, 8). For viral fusion proteins in the so-called "class I" category, the arms of the prehairpin intermediates are each trihelical bundles designated as heptad repeats 1 and 2 (HR1 and HR2), and closure to the postfusion state therefore creates six-helix bundles (6-HBs) of antiparallel HR1 and -2 segments, with FPs abutted next to transmembrane (TM) spans in the coalesced membrane (see Fig. 6 for a depiction of this process). Viral fusion proteins in other classes go through related refoldings to effect membrane coalescence, but the hairpin arms are not necessarily α-helical (1).

Although this view of viral protein-mediated membrane fusion is satisfying in many ways, important details are missing. For example, the importance of the TM and endodomain (ENDO) portions of the surface proteins demand more prominent attention in the membrane fusion models. Because these TM and ENDO regions are not structurally resolved, it can be difficult to accurately add them into the models. However, abundant literature indicates that TM-ENDO portions of many different virus fusion proteins do operate to control virus-cell and cell-cell fusion (9–12). An influenza hemagglutinin fusion protein with a glycosylphosphatidylinositol anchor replacing its TM-ENDO domains was able to mediate outer membrane leaflet fusions (*i.e.* hemifusion) but could not create full membrane fusions (13). The animal retrovirus envelope proteins contain long ENDO domains that include the "R peptides" that, once removed by proteolysis, facilitate the fusion reaction (14, 15). Truncation of the human immunodeficiency virus (HIV) envelope ENDO tail modulates its fusogenicity (16). Finally, it is notable that many viral fusion protein ectodomain fragments lacking TM and ENDO domains fold into postfusion states (17, 18), suggesting that membrane-anchoring parts help maintain functional metastable high energy conformations.

It is not entirely clear how the intravirion parts of the fusion protein influence reactions that are carried out by the much

* This work was supported, in whole or in part, by National Institutes of Health Grant R01 AI60030.

[1] To whom correspondence should be addressed: Dept. of Microbiology and Immunology, Loyola University Medical Center, 2160 S. First Ave., Maywood, IL 60153. Tel.: 708-216-4850; Fax: 708-216-9574; E-mail: tgallag@lumc.edu.

[2] The abbreviations used are: FP, fusion peptide; MHV, mouse hepatitis virus; HR, heptad repeat; 6-HB, six-helix bundle; TM, transmembrane; ENDO, endodomain; HIV, human immunodeficiency virus; CoV, coronavirus; SARS, severe acute respiratory syndrome; DMEM, Dulbecco's modified Eagle's medium; FBS, fetal bovine serum; mAb, monoclonal antibody; rA59, recombinant A59; WT, wild type; S, spike; M, membrane.

larger exterior portion of the protein. We and others consider it plausible that changes in the fusion protein endodomain impact refolding rates, which in turn control the route and timing of virus entry. This is because the transitions from prehairpin intermediate to postfusion states require large scale transit of TM-ENDO domains across lipid stalks (19), which may be a rate-limiting step in the process.

We investigate the cell entry of coronaviruses (CoVs). The CoVs are enveloped, plus-strand RNA viruses causing respiratory and gastrointestinal diseases in animals and humans. The prototype human pathogenic CoV is severe acute respiratory syndrome (SARS)-CoV (20). We have found that the CoVs provide a good model in which one can study the relationship between endodomain changes and fusion reaction kinetics. CoV spike (S) proteins are solely sufficient to mediate virus-cell fusion and cell entry. The S protein ectodomains are trimers (21) with classical "class I" fusion protein characteristics (22). The relative positions of fusion peptides (23), HR regions (24, 25), and TM span are known, and condensed six-helix bundles of antiparallel HR1 and HR2 have been crystallographically resolved (26, 27) (see Fig. 1). The S protein endodomains comprising the carboxyl termini are set apart by their abundance of cysteine residues. Many if not all of these cysteines are well known to be post-translationally acylated with palmitate and/or stearate adducts (28–31); these post-translational modifications add considerable lipophilicity to the endodomains and probably position the ENDO tails against the inner face of virion membranes. Indeed, the S proteins are set apart from other enveloped virus glycoproteins in having very richly acylated endodomains. There are nine acylated cysteines in coronavirus S, whereas there are only three in influenza HA (32) and two in HIV gp160 (33). Interference with S endodomain palmitoylation, either by engineered mutations or pharmacologic agents, diminishes or eliminates S-mediated membrane fusion activities (28, 29, 31, 34), but the mechanisms by which these endodomain alterations influence membrane fusion activities are unknown.

Here we explore the mechanistic basis for these observations. Our findings indicate that spikes harboring endodomain cysteine mutations can fold into prefusion forms, can reach infected cell surfaces, and can mediate cell-cell fusions. However, the endodomain mutant spikes that we evaluate here cannot efficiently incorporate into secreted virions, and those few that do incorporate into virions cannot efficiently support virus-cell entry and fusion because they are slow at refolding into postfusion forms. We interpret these findings in the context of the class I protein-mediated membrane fusion pathway and suggest that endodomain palmitates serve to anchor spike protein trimers onto virion membranes such that metastable prefusion spike conformations can be maintained and also progress through conformational intermediates in a timely fashion.

EXPERIMENTAL PROCEDURES

Cells—Murine 17cl1 fibroblasts (35) were grown in Dulbecco's modified Eagle's medium (DMEM) containing 5% tryptose phosphate broth (Difco) and 5% heat-inactivated fetal bovine serum (FBS). 293T, FCWF (36), and HeLa-CEACAM (carcinoembryonic antigen cell adhesion molecule isoform 1a; cell line number 3) cells (37) were grown in DMEM supplemented with 10% FBS. All growth media were buffered with 0.01 M sodium HEPES (pH 7.4).

Plasmid DNAs—MHV-A59 S and M cDNAs were PCR-amplified using template pMH54-A59 (38, 39) and cloned into pCAGGS.MCS (40) between SacI and XmaI restriction sites. Mutations in the pCAGGS-S construct were created using mutagenic primers and a site-directed mutagenesis protocol. (QuikChange® XL; catalogue number 200519-5; Stratagene). All plasmid constructs were sequenced to confirm the presence of desired mutations. Primers and primer sequences are available upon request.

Recombinant Viruses—Recombinant MHVs were created via targeted RNA recombination (39). Mutations in the pMH54-E-FL-M construct (41) were created using site-directed mutagenesis, as described above. The plasmid DNAs were linearized by digestion with PacI and used as templates for *in vitro* transcription reactions using T7 RNA polymerase and reagents from Ambion (mMESSAGE mMACHINE®; catalogue number AM1344). Transcripts were electroporated into $\sim 10^7$ feline FCWF cells that were infected 4 h earlier with recombinant coronavirus feline MHV-A59 (39), using a Bio-Rad Gene Pulser II. The electroporated FCWF cells were added to a monolayer of $\sim 10^6$ 17cl1 cells. Recombinant viruses, identified by syncytia development on 17cl1 cells, were then collected from media and isolated by three cycles of plaque purification on 17cl1 cells. Mutations fixed into the recombinant MHVs were confirmed by reverse transcription PCR and sequencing. Sequence determinations included ~300 nucleotides spanning the intended site-directed mutations.

Radiolabeling and Virus Purification—Viruses were adsorbed to 17cl1 cells at a multiplicity of infection of 1 for 1 h at 37 °C in serum-free DMEM and then aspirated and replaced with DMEM supplemented with 5% FBS. At 12 h postinfection, media were removed, and cells were rinsed extensively with saline. For radiolabeling with ^{35}S-labeled amino acids, cells were first incubated for 30 min at 37 °C in labeling medium (methionine- and cysteine-free DMEM containing 1% dialyzed FBS). The cells were then replenished with labeling medium containing 60 μCi/ml Tran ^{35}S-label (MP Biomedicals, Irvine, CA), and incubated for 4 h at 37 °C. Media collected from infected cell cultures were centrifuged for 10 min at 2,000 × *g* and then for 20 min at 20,000 × *g* and then overlaid on top of discontinuous sucrose gradients consisting of 5 ml of 30% and 2 ml of 50% (w/w) sucrose in HNB buffer (50 mM HEPES (pH 7.4), 100 mM NaCl, 0.01% bovine serum albumin). Virions were equilibrated at the 30–50% sucrose interface, using a Beckman Spinco SW41 rotor at 40,000 rpm for 2 h at 4 °C and recovered by fractionation from air-gradient interfaces.

Immunoprecipitations and Immunoblotting—293T cells were co-transfected via calcium phosphate (42, 43) with pCAGGS-M and pCAGGS-S constructs. At 40 h post-transfection, the cell monolayers were lysed in HNB buffer containing 0.5% Nonidet P-40, 0.5% sodium deoxycholate, and 0.1% protease inhibitor (Sigma P2714). Cell lysates were first clarified by centrifugation at 2,000 × *g* for 5 min, and then 160,000 cell equivalents were mixed with 0.01 ml of 1 mg/ml

N-CEACAM-Fc (44) and 0.06 ml of protein G magnetic beads (NEB Corp., Inc.) for 2 h at 25 °C. Beads were rinsed three times with HNB buffer containing 0.5% Nonidet P-40, 0.5% sodium deoxycholate. Proteins were eluted from beads by the addition of electrophoresis sample buffer (0.125 M Tris (pH 6.8), 10% dithiothreitol, 2% SDS, 10% sucrose, 0.004% bromphenol blue) and heating to 95 °C for 5 min and subsequently subjected to SDS-PAGE. SDS gels were transferred to polyvinylidene difluoride membranes that were subsequently blocked for 1 h with 5% nonfat milk powder in TBS-T (25 mM Tris-HCl (pH 7.5), 140 mM NaCl, 2.7 mM KCl, 0.05% Tween 20). S proteins were detected with murine mAb 10G (45) (1:2000 in TBS-T). M proteins were detected with murine mAb J.3.1 (46) (1:500 in TBS-T).

Pseudotyped Virions and Transductions—To generate pseudotyped HIV particles, 293T cells were co-transfected via calcium phosphate (42, 43) with pNL4.3-Luc R-E- (National Institutes of Health AIDS Research and Reference Program number 3418) and the various pCAGGS-S constructs. After 2 days, media were collected, clarified for 10 min at 2,000 × *g*, and then overlaid on top of a 30% sucrose cushion in HNB buffer and centrifuged at 40,000 rpm for 2 h at 4 °C using a Beckman SW41 rotor. Pelleted particles were resuspended in HNB buffer and stored at −80 °C. For biochemical analysis, pelleted HIV pseudoparticles were resuspended in electrophoresis sample buffer and processed by immunoblotting as described above. S proteins were detected with murine mAb 10G (45) (1:2,000 in TBS-T). HIV capsid protein (p24) was detected with murine mAb αp24 (National Institutes of Health AIDS Research and Reference Program) (1:5000 in TBS-T). For transductions, HIV particles, normalized to p24 levels, were adsorbed to HeLa-CEACAM cells in serum-free DMEM for 2 h. Subsequently, the inoculum was removed and replaced with DMEM supplemented with 10% FBS.

At 2 days post-transduction, the cells were rinsed with saline and dissolved in luciferase lysis buffer (Promega E397A). Luminescence was measured upon the addition of luciferase substrate (Promega E1501) using a Veritas microplate luminometer (Turner BioSystems). In some experiments, HR2 peptide (25 μM) was added as indicated under "Results."

Protease Digestion Assay—For the protease digestion assay (47), 10^4 plaque-forming units of recombinant A59 (rA59) coronavirus in 20 μl of DMEM supplemented with 5% FBS or HIV pseudoparticles in 20 μl of HNB buffer were incubated with N-CEACAM-Fc (2 μM) for various times at 37 °C. After samples were placed on ice for 10 min, proteinase K (Sigma) was added at a final concentration of 10 μg/ml, and digestion was carried out at 4 °C for 20 min. Reactions were terminated by the addition of electrophoresis sample buffer and subjected to SDS-PAGE and immunoblotting as described above.

Cell-Cell Fusion Assay—Cell-cell fusion was performed as described previously (48). Briefly, effector cells (HeLa) were transiently transfected with a pCAGGS vector encoding T7 polymerase and the various pCAGGS-S constructs using Lipofectamine 2000 reagent (Invitrogen). Target cells were generated by Lipofectamine transfection of HeLa-CEACAM cells with pT7pro-EMC-luc, which encodes firefly luciferase under T7 promoter control (49). At ~6 h post-transfection, the target cells were quickly trypsinized and added to adherent effector cells in a 1:1 effector/target cell ratio. After a ~4-h co-cultivation period, luciferase levels were quantified as described above.

RESULTS

Effect of Endodomain Mutations on S Incorporation into Virions—The MHV strain A59 S protein has nine cytoplasmic (endodomain) cysteines, most or all of which are known to be stably thioacylated with palmitic acids (28–31) We mutated those most distal from the transmembrane span, the carboxyl-terminal Cys^{1300}, Cys^{1303}, and Cys^{1304}, to alanines, with the expectation that these changes would prevent S palmitoylation at these positions and thus untether the ends of the S tails from cytosolic membrane faces (Fig. 1*A*). Our goal was to discern the functional consequences of these changes. To this end, we used targeted RNA recombination to direct mutations into the MHV genome, thus creating a series of recombinant MHV viruses harboring cysteine-to-alanine substitutions. The parent virus we used is a recombinant MHV-A59 strain engineered to produce firefly luciferase, identical to that developed by de Haan *et al.* (50).

Biochemical evaluation of the newly generated recombinant viruses involved ^{35}S radiolabeling of infected 17cl1 cell monolayers. ^{35}S-virions were harvested from culture media, purified by density gradient ultracentrifugation, and evaluated for radioactive protein content by SDS-PAGE and autoradiography. The single mutant C1304A recombinant virions were indistinguishable from WT rA59 in these electrophoretic analyses (data not shown). Fig. 2*A* depicts the virion proteins associated with wild type (WT) rA59 in comparison with C1303A/C1304A rA59. The C1303A/C1304A mutant virions were noticeably depleted in S protein content (11-fold relative to WT). The triple mutant C1300A/C1303A/C1304A recombinant viruses were never isolated despite several attempts, suggesting that a threshold of spike density is required for virus viability.

An explanation for the reduced incorporation of endodomain mutant spikes into virions appeals to disruption of S protein interaction with M proteins, the M proteins being the key orchestrating agents in the virion assembly process (51, 52). Thus, we co-expressed the various spike constructs individually with M protein in 293T cells and subsequently dissolved cell monolayers in a buffer containing both Nonidet P-40 and sodium deoxycholate, a detergent formulation known to preserve association between S and M proteins (53). S·M complexes were captured using the S-binding immunoadhesin N-CEACAM-Fc (44) and magnetic protein G beads. Eluted proteins were detected by Western blot using anti-S and anti-M antibodies, and the results (Fig. 2*B*) revealed that the poor incorporation of endodomain mutant spikes into recombinant virions correlated with their failure to efficiently associate with M proteins.

Effect of Endodomain Mutations on Spike-mediated Membrane Fusion—To investigate the role of endodomain cysteines on the membrane fusion reaction, we first performed cell-cell fusion assays. To this end, cells transfected with various pCAGGS-spike constructs were co-cultivated with target cells containing murine CEACAMs, the primary MHV receptors.

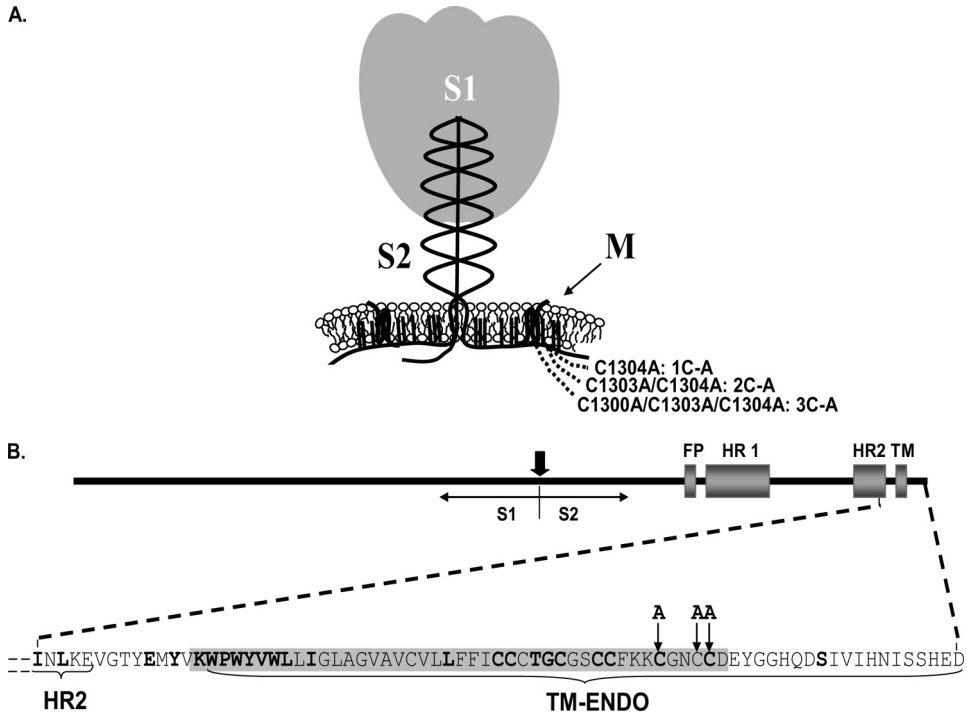

FIGURE 1. **Schematic representation of the MHV-A59 S protein.** *A*, the S trimer is depicted as peripheral S1 and integral membrane S2 subunits. The S2 subunits are drawn in the context of a virion membrane and in association with M proteins. Endodomain mutations preventing S acylation are illustrated on one S2 monomer. Loss of palmitoylation and the hypothetical untethering of cytoplasmic tails from intravirion membrane leaflets are depicted by the *dotted lines*. *B*, a linear map of the MHV-A59 S protein is shown. The *thick arrowhead* marks the furin cleavage site separating S1 and S2. On the S2 portion, the FP, HR1, HR2, and TM region are indicated by the *shaded boxes*. Amino acid sequences from Ile^{1250} to the carboxyl terminus are presented, and the predicted α-helical region (Lys^{1263}–Asp^{1305}) is shown *highlighted* in *gray*. S sequences from viruses in antigenic groups I (human coronavirus NL63, transmissible gastroenteritis virus), II (mouse hepatitis virus strain A59, severe acute respiratory syndrome coronavirus), and III (infectious bronchitis virus, turkey coronavirus) were aligned, and residues conserved in at least four of the six are indicated by *boldface letters* in the amino acid sequence. *Thin arrows* mark the cysteines that were mutated in this study.

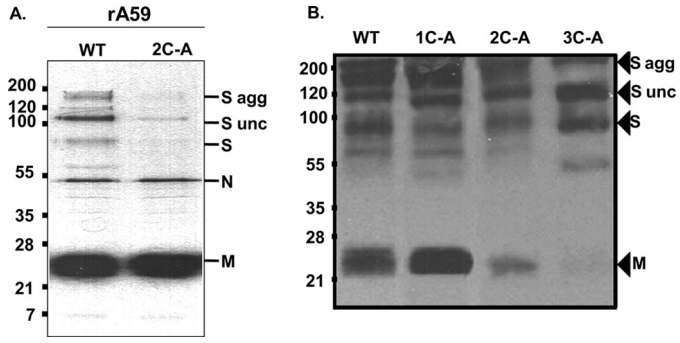

FIGURE 2. **Effect of S endodomain cysteine mutations on virion incorporation and association with M proteins.** *A*, recombinant virions were metabolically radiolabeled with ^{35}S-amino acids and purified by sucrose density gradient ultracentrifugation. Equal ^{35}S radioactivities were collected from each purified virion preparation, electrophoresed on SDS gels, and detected by autoradiography. *S agg*, S aggregates; *S unc*, uncleaved S; *N*, nucleocapsid protein; *M*, membrane protein. Molecular masses are shown in kilodaltons. *B*, 293T cells co-expressing the indicated S constructs with M proteins were dissolved in Nonidet P-40/deoxycholate buffer, and S·M complexes were captured using an MHV-soluble receptor immunoadhesin (nCEACAM-Fc) bound to magnetic protein G beads. Eluted proteins were detected by Western immunoblotting using S- and M-specific mAbs. *1C-A*, C1304A; *2C-A*, C1303A/C1304A; *3C-A*, C1300A/C1303A/C1304A.

Spike-bearing cells contained phage T7 polymerase, and CEACAM cells harbored luciferase genes whose transcription required the T7 polymerases, making it so that luciferase enzyme activities increased in response to spike-induced cell-cell fusions. From these assays, we found that all spikes induced similar luciferase accumulations (Fig. 3*A*). Thus, at least within a 4-h cell co-cultivation period, the various endodomain mutant spikes were equivalent in cell-cell fusion activities.

An inference from the results of cell-cell fusion assays is that the various spike proteins accumulate equivalently on cell surfaces. If so, then the spike proteins might incorporate equivalently onto HIV virus cores budding from plasma membrane sites, making HIV-coronavirus S pseudoparticles appropriate for virus-cell fusion assays. Such HIV-S pseudoviruses could replace authentic rA59 coronaviruses for use in virus-cell fusion assays, the rA59 viruses being unsuitable for correlating endodomain changes with virus-cell fusion because of the confounding effect of these endodomain changes on the assembly of spikes into virions (Fig. 2*A*).

HIV-CoV S pseudotype virions were produced by co-transfecting 293 cells with an envelope-deficient HIV vector (pNL4-3-Luc-R-E) along with pCAGGS-S constructs. Released pseudoparticles were harvested from culture media, purified by sucrose gradient ultracentrifugation, and subjected to SDS-PAGE. The data (Fig. 3*B*) revealed that WT and endodomain mutant spikes did indeed incorporate onto HIV particles with equal efficiencies. However, when the HIV-S particles were used to transduce CEACAM receptor-bearing target cells, the single (C1304A) double (C1303A/C1304A), and triple (C1300A/C1303A/C1304A) cysteine mutants were about 2, 20, and 40 times less efficient at delivering the HIV cores into cells, as measured by a luciferase reporter that is part of the recombinant HIV genome (Fig. 3*C*). These data indicate that endodomain cysteines and most likely their palmitate adducts are specifically needed to facilitate effective virus-cell fusion.

We wanted to investigate the mechanism by which these endodomain mutations suppressed virus entry. One possibility is that S-mediated entry was impaired because endodomain mutations reduced the affinity of S ectodomains for CEACAM receptors. To address this speculation, we produced highly purified ^{35}S-labeled WT and C1303A/C1304A rA59 virions and assessed their immunoprecipitation with N-CEACAM-Fc. In 1-h, 4 °C incubation periods, the ^{35}S radioactivities that were captured varied by $<$10% between WT and C1303A/C1304A virions. Furthermore, we observed no significant differences in the association of ^{35}S-labeled WT and Cys → Ala pseudovirions with CEACAM-bearing host cells (data not shown).

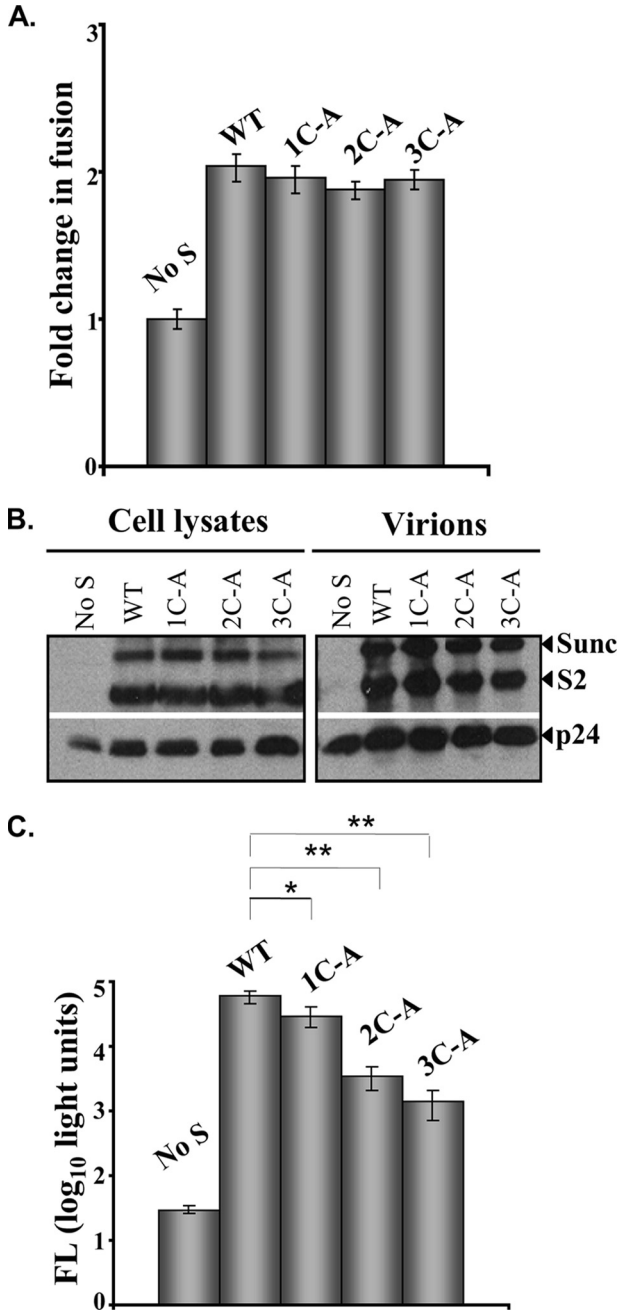

FIGURE 3. **Analysis of coronavirus S-mediated fusion and transduction potentials.** *A*, the indicated S proteins were evaluated using assays involving luciferase reporter gene expressions as readouts of cell-cell fusion. Luciferase readings made 4 h after co-cultivation with fusion targets are plotted as -fold change in fusion over the negative control lacking spike proteins. *B*, pseudotyped HIV particles were produced in 293T cells by co-transfection of plasmid DNAs encoding the indicated spikes together with the HIV vector (pNL4.3-Luc R-E-). Released particles were harvested from culture media and concentrated by pelleting through 30% sucrose. Proteins present in cell lysates and in virion particles were detected by immunoblotting using S- and p24-specific mAbs. *C*, HIV particles normalized to p24 content were used to transduce HeLa-CEACAM cells. Two days post-transduction, the cells were lysed, and luciferase activities were assayed as described under "Experimental Procedures." *, $p < 0.05$; **, $p < 0.002$ (Student's *t* test for independent samples). *1C-A*, C1304A; *2C-A*, C1303A/C1304A; *3C-A*, C1300A/C1303A/C1304A.

Given that the endodomain mutations had no obvious effect on receptor interactions, their suppression of virus entry was probably at the level of membrane fusion. To address this possibility and evaluate S-mediated fusion in detail, we monitored S protein refolding events with an HR2 peptide that was previously shown to be a potent fusion inhibitor (22). The HR2 peptide used (NVTFLDLTYEMNRIQDAIKKLNESYINLKE) corresponds to residues 1225–1254 of the MHV strain A59 spike. The view is that HR2 peptides bind exposed HR1 trimers, thereby occluding the *cis* refolding of endogenous HR2 helices onto HR1, preventing 6-HB formation, membrane fusion, and virus entry (54, 55). These exposed HR1 trimers are present only in transitional S protein folding states; in support of this statement, we found that HR2 peptides could be incubated indefinitely with virions at 50 μM (50 × EC_{50}) (56) at 37 °C, and after diluting to 0.5 nM (0.0005 x EC_{50}), they effect no inhibition of plaque development.

In our experiments, we used the HR2 peptide as a tool to monitor the exposure of HR1 (reflecting S unfolding) and subsequent disappearance of HR1 (reflecting S refolding into post-fusion 6-HBs) during virus entry into cells. In this experimental design, we applied HIV-S pseudoparticles to CEACAM-bearing HeLa cells at 4 °C and incubated to equilibrium. Unbound particles were aspirated and replaced with prewarmed 37 °C media, because the 37 °C temperature is required for fusion and for S protein conformational changes (57, 58). Then the HR2 peptide (25 μM) was added at the 37 °C temperature shift and subsequently removed at 0-, 2-, 4-, 8-, 16-, 32-, and 64-min time intervals (Fig. 4*A*) or added at early 0-, 2-, 4-, 8-, 16-, 32-, and 64-min time intervals after the temperature shift (Fig. 4*B*). At the 64 min time point, all cells were rinsed, replenished with complete media, and then assayed 40 h later for accumulated luciferase, which served as the readout for S-mediated psuedovirus entry.

When HR2 peptide was present from 0 to 64 min after the 37 °C temperature shift, WT S-mediated infection was blocked by more than 1,000-fold (Fig. 4*B*). However, when HR2 peptide was present from 2 to 64 min, blockade was only about 20-fold, suggesting that ~5% of the entry-related WT S protein refolding events took place within the first 2 min after 37 °C temperature shift. When HR2 was added after 16 min at 37 °C, blockade was only 2–3-fold, again suggesting that ~30–50% of entry was completed within 16 min. Quite strikingly, and in sharp contrast to the rapid refolding of the wild type S proteins, the single (C1304A), double (C1303A/C1304A), and triple (C1300A/C1303A/C1304A) endodomain mutant pseudoviruses were more sensitive to inhibition by HR2 peptides added late after 37 °C temperature shift, with the extent of this sensitivity to HR2 inhibition correlating directly with the degree of Cys → Ala substitution. Entry mediated by the triple mutant S proteins was completely inhibited by HR2 peptides added as late as 16 min after the 37 °C shift, suggesting that the HR1 trihelix exposed itself in delayed fashion and/or remained exposed for remarkably prolonged periods in relation to the wild type protein. A reasonable speculation is that this slower fusion kinetics accounted for the general inefficiencies of the endodomain-mutant S proteins in mediating virus entry (Fig. 3*C*). This same degree of slower fusion kinetics is not revealed by the much longer 4-h cell-cell fusion assay (Fig. 3*A*).

The kinetics of S protein refolding was further examined using a biochemical approach. A distinct experimental advan-

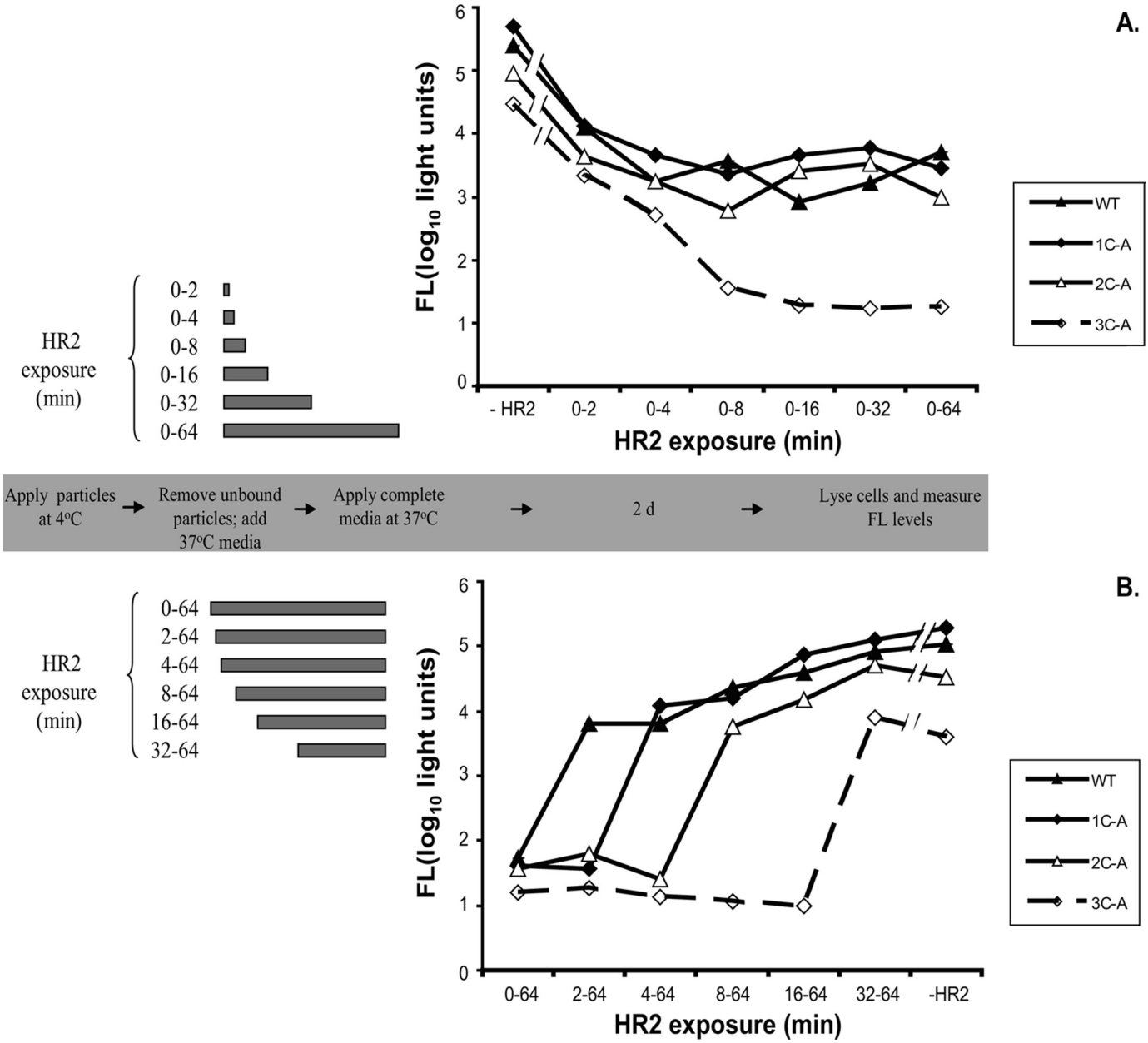

FIGURE 4. **Time course of entrance into and exit from HR2-sensitive folding states.** HIV particles normalized to p24 content were prebound to HeLa-CEACAM cells at 4 °C for 1 h. Unbound particles were then aspirated, and 37 °C serum-free DMEM with or without HR2 peptide (25 μM) was added to the cells. The HR2 peptides were subsequently removed at 0-, 2-, 4-, 8-, 16-, and 32-min time intervals (*A*) or added at 0-, 2-, 4-, 8-, 16-, and 32-min time intervals after the temperature shift (*B*). At the 64 min time point, all cells were rinsed and replenished with DMEM supplemented with 10% FBS, and luciferase accumulations were assayed 2 days post-transduction. *1C-A*, C1304A; *2C-A*, C1303A/C1304A; *3C-A*, C1300A/C1303A/C1304A.

tage of the coronaviruses is that their S proteins can be triggered to refold into 6-HBs in reductionist *in vitro* assays by relatively simple exposure to soluble receptors at 37 °C temperature (47, 57). The resulting 6-HBs, being extraordinarily stable (59), can be visualized in Western blots as ~58 kDa protease-resistant bands (47). We incubated wild-type and double cysteine mutant (C1303A/C1304A) virions with soluble receptor (N-CEACAM-Fc) at 4 °C and, once at equilibrium, shifted to 37 °C for various time periods. Increased levels of 6-HBs were observed with 37 °C incubation time (Fig. 5*A*). Far more striking was the finding that the endodomain mutant C1303A/C1304A S proteins were less prone to advancing into 6-HB configurations (Fig. 5*A*). Similar experiments performed with HIV-S pseudoviruses generated corroborating findings of diminished 6-HBs in C1303A/C1304A and C1300A/C1303A/C1304A S proteins (Fig. 5*B*). The distal carboxyl-terminal cysteines and/or their palmitate adducts increase the facility of S-mediated refolding into postfusion forms.

DISCUSSION

Viral fusion proteins have distinctive, sequence-specific TM and ENDO domains. Deleting or replacing these regions with similar hydrophobic sequences can eliminate fusion function (60 – 64). Sequence specificity indicates that the TM and ENDO domains have functions beyond mere anchoring of their respective ECTO domains. During membrane fusion, the TM

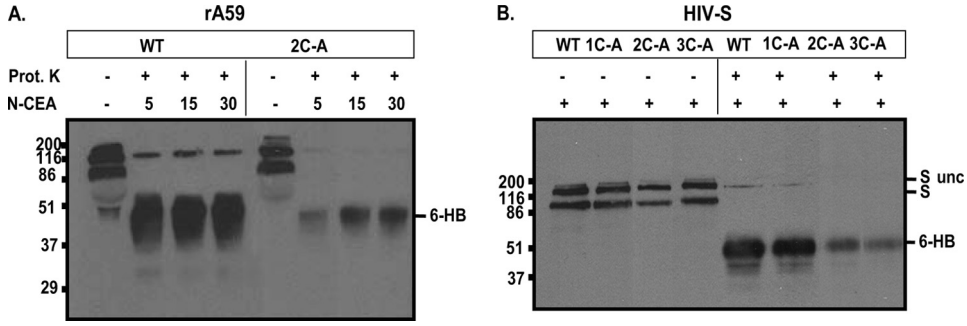

FIGURE 5. **Effect of endodomain cysteine mutations on the formation of postfusion 6-HB hairpin conformations.** *A*, wild-type and double cysteine mutant (C1303A/C1304A) rA59 viruses in DMEM supplemented with 5% FBS were incubated with 2 μM soluble receptor (N-CEACAM-Fc) at 37 °C for 5, 15, or 30 min. Subsequently, proteinase K (*Prot. K*) was added to the indicated samples (final concentration 10 μg/ml), and all reactions were incubated for 15 min at 4 °C. The protease digestion was halted by the addition of electrophoresis sample buffer, and samples were immediately subjected to Western immunoblotting. *S unc*, uncleaved S; *6-HB*, protease-resistant 6-HB. Molecular masses are shown in kilodaltons. *B*, concentrated HIV particles in HNB buffer were incubated with 2 μM soluble receptor for 5 min at 37 °C. Proteinase K digestion, quenching, and immunoblotting were performed as described above. *1C-A*, C1304A; *2C-A*, C1303A/C1304A; *3C-A*, C1300A/C1303A/C1304A.

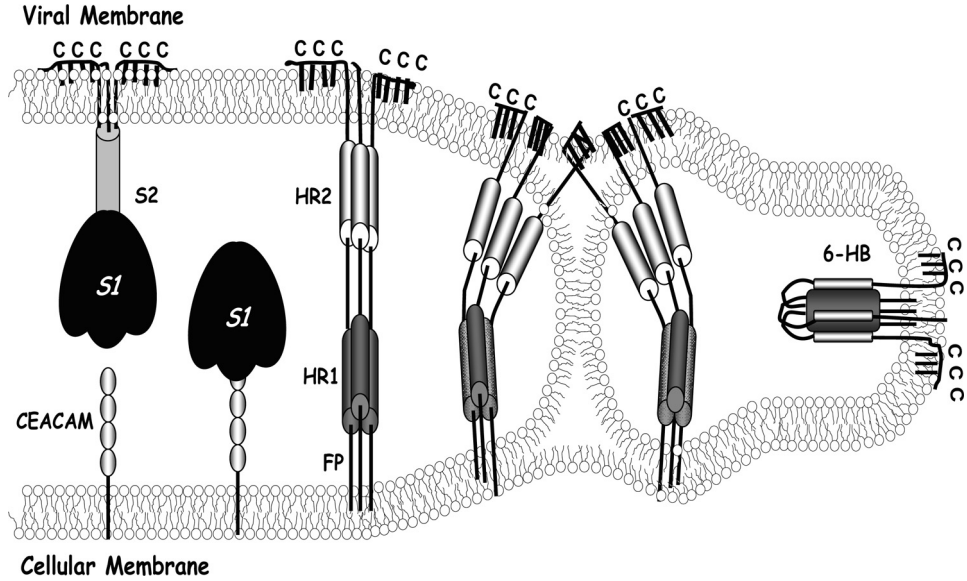

FIGURE 6. **Coronavirus S protein-mediated membrane fusion model.** A hypothetical depiction of the native prefusion S protein (*left*) is depicted binding to cellular CEACAM receptors. S1 subunit dissociation and S2 unfolding generates prehairpin structures (*middle*) depicted with cell membrane-intercalated FPs and exposed heptad repeat regions (HR1 and -2). Prehairpin closure through a lipid stalk intermediate generates a highly stable, rodlike 6-HB, in which HR2 helices are positioned antiparallel to an interior HR1 trimer. Palmitates are shown extending from endodomain cysteines (*C*).

spans transit through hemifusion "lipid stalk" structures, and in postfusion states, the TM spans link stably onto FPs (6, 65) (also see Fig. 6). In addition to amino acid sequence specificities, the TM spans of viral fusion proteins appear to have unusual length requirements as well. Whereas a 20-residue α helix can vertically span a lipid bilayer, viral fusion proteins have hydrophobic, putative TM spans ranging from ~25 to ~50 residues. There are several proposed operating mechanisms for these lengthy hydrophobic helices. One view is that the long hydrophobic stretches, if positioned during prefusion states at oblique angles relative to effector membrane planes, might create membrane deformations or dimples that facilitate transitions into lipid stalk conformations (19, 66). Another superior viewpoint is that long hydrophobic anchoring helices are required so that they can be accommodated at various orientations within the curved membrane architectures arising during bilayer fusions (9) (also see Fig. 6). Last, anchoring motifs may operate at the latest fusion stages to ensure that the transit of TM spans through lipid stalks comes concomitant with complete bilayer fusions (19).

We performed this research out of our understanding that coronavirus S proteins have distinctive TM-ENDO domain features that might further reveal fusion operating mechanisms. The portion of the coronavirus TM-ENDO region that is highly hydrophobic and probably α-helical includes ~42 amino acids, from Lys^{1263} to Asp^{1305}, in MHV A59 (see Fig. 1*B*). The COOH-terminal part of this region comprises the cysteine-rich motif, and if all cysteines are palmitoylated, as is strongly suggested by [^{3}H]palmitate labeling (28, 30), then this region would be extraordinarily lipophilic. Indeed, each S trimer would add 27 16-carbon acyl chain lipids to the intravirion membrane leaflet. Several reports evaluating truncated coronavirus S proteins missing part or all of these acylated tails have provided valuable data on the minimal tail lengths required to preserve biological function (28, 30, 67, 68). We used a more subtle approach to evaluate tail activities by substituting one or more of the nine cysteines in the palmitoylation motif with alanines. We expected that the reduced palmitoylation in the Cys → Ala mutants would have deleterious effects on membrane fusion, in accordance with earlier reports (28), but would not entirely eliminate fusion activities in the way that the truncation mutants do, making it so that we could gain some insights into the specific points in the fusion reaction where the palmitates might be operating.

One of our findings was that the distal cysteine-to-alanine substitutions in the endodomain reduced spike protein incorporation into virions. Hydrophobic palmitates may determine assembly of spike into virus particles by helping position the endodomain along the cytoplasmic face of lipid bilayers, thereby facilitating interaction with the assembly-orchestrating M protein. It has already been established that the S-M interaction is generally dependent on S protein palmitoylation, since the addition of a pharmacologic inhibitor of palmitoylation (2-bromopalmitate) inhibits efficient S·M complex formation (29). This report indicates that the most distal carboxyl-termi-

nal cysteines/palmitates are crucial elements for S incorporation. Notably, for other class I fusion proteins, such as HIV-1 Env and influenza HA, palmitoylation of endodomain cysteines is also required for assembly (69, 70), although these requirements vary with influenza virus strains. For HIV and influenza, assembly and budding take place at or near the plasma membrane in lipid raft microdomains (71, 72), and the requirements for glycoprotein incorporation into virions might be explained by the biophysical partitioning of palmitoylated proteins into lipid rafts (73). Coronaviruses bud into the ER (74, 75), where raft-defining lipids are relatively rare (76). Thus, the palmitate requirements for S assembly are less clear, but it is possible that the extraordinary degree of S palmitoylation organizes adjacent ER lipids into rigid arrays that are akin to raftlike environments. Indeed, if the endodomains are α-helical, as predicted by bioinformatics, then palmitates extending from cysteines spaced 3–4 residues apart would be within ~5 Å of each other, forming nanoarrays of adjacent saturated fatty acids underneath each S trimer. This hypothetical lipid organization around S proteins might create ER membrane environments that are crucial to coronavirus assembly. The next step in understanding assembly may come in dissecting viral protein-lipid and lipid-lipid interactions.

There were direct relationships between S assembly and S-mediated membrane fusion competence. For example, relative to wild-type S, the C1303A/C1304A mutant was poorly incorporated into virions (Fig. 2*A*) and was a compromised membrane fusogen (Figs. 3*C* and 4). These relationships argue for a sorting process at the budding sites, with inclusion of S proteins into virions according to palmitoylation status. This sorting process insures that only the most palmitoylated, fastest fusing S proteins are integrated into secreted virions. S proteins with less palmitoylation sort to cell surfaces as free proteins and perform related cell-cell fusions. This cell-cell fusion activity appears to be far less dependent on quick fusion reactions because the wild type and Cys → Ala mutants were indistinguishable in our assays of syncytial formation (Fig. 3*A*).

On cell surfaces, the wild type and Cys → Ala mutant S proteins probably occupy similar raftlike environments, because all S forms were equally incorporated into the HIV-based pseudoviruses that are known to bud from lipid raft microdomains (77) (Fig. 3*B*). Using these HIV-S pseudoviruses, we found that the stepwise substitution of one, two, and then three COOH-terminal cysteines caused progressively declining transduction. This result could not be explained by any obvious defects in S protein structure or density on pseudoviruses because uncleaved and cleaved S forms were equally abundant in all viruses (Fig. 3*B*). Therefore, we sought out more subtle effects of the endodomain mutations on the virus entry process by using HR2 peptides, potent inhibitors of virus entry, as probes for the intermediate folded S protein conformations (Fig. 4). By adding HR2 peptides into media at various times before and after initiating the S refolding reaction, we could assess the time required for S proteins to enter into and out of the intermediate prehairpin state (see Fig. 6). These experiments yielded enlightening results, allowing us to conclude that the endodomain mutants remained HR2-sensitive for prolonged periods, in essence slowing the kinetics of refolding relative to wild type S proteins.

Endodomain mutant S proteins transition from native to unfolded prehairpin states at the same rate as wild type spikes, because HR2 peptides added 0–2 min after initiating S refolding resulted in a ~10-fold reduction for all S-mediated transductions (Fig. 4*A*). Similarly, equivalent inhibitions were observed when HR2 peptides were added 0–4 min after initiation. In contrast, when HR2s were introduced at various times after initiating S refoldings, the Cys → Ala mutants were preferentially blocked (Fig. 4*B*). These data support a view in which the duration of the prehairpin state is regulated by the palmitoylated endodomains. We consider it likely that virus S proteins are triggered to unfold into the prehairpin (HR2-sensitive) state at cell surfaces, immediately after binding cell surface CEACAM receptors. Particularly for those viruses with underpalmitoylated S proteins, we suggest that this prephairpin architecture remains as viruses enter endosomes, whereupon all but the core HR1-HR2 fusion machinery is cleaved away by endosomal proteases (4, 78). Following this proteolysis, hairpin closure might then ensue, effecting the membrane fusion event. The timely completion of this hairpin closure appears to be correlated with virus infectivity.

As we expected, the kinetics of S protein refolding was also reflected by the relative abundances of proteinase K-resistant 6-HB hairpin forms in the various virus preparations. Our experiments here were modeled after those of Taguchi *et al.* (47), who found that coronavirus S proteins can be triggered to refold into 6-HBs by exposure to soluble receptors. Indeed, soluble receptors created increasing 6-HB levels with increasing incubation time (Fig. 5*A*), and the endodomain mutations impeded this 6-HB formation in accordance with the number of endodomain mutations (Fig. 5*B*).

All of these findings solicit speculations on the way in which the endodomains, specifically the cysteines and/or their palmitate adducts, change the rate-limiting step of the membrane fusion reaction. Given that the endodomain Cys → Ala mutations progressively extend the HR2-sensitive stage, we suggest that the absence of these cysteines-palmitates raises an activation energy barrier between the HR2-sensitive and 6-HB stage. It was recently discovered that the SARS-CoV HR2 regions exist in a monomer-trimer equilibrium (79). The idea is that the equilibrium has to be shifted toward monomers, so that separated HR2 helices can each invert relative to HR1 and attach in antiparallel fashion onto the HR1 trimers (see Fig. 6). Given that the HR2 regions in isolation can stick together into trimers (79), the role of the endodomain cysteines-palmitates could be to anchor the transmembrane spans such that a separation of HR2 monomers is maintained in the native S structure. This prevention of HR2 trimerization in the native structure would then allow membrane fusion to occur in a timely fashion. We take our cues here from the cryoelectron microscopy reconstructions of HIV that reveal a tripod-like arrangement for virus spikes coming out of the virion membrane (80, 81). Class I protein-mediated membrane fusion may depend on prefusion spikes with separated HR2 domains. Palmitoylation of juxtamembranous cysteines may induce the transmembrane domain to tilt relative to the lipid bilayer plane, as suggested by

Abrami *et al.* (82), who found that unusually long transmembrane spans could be accommodated within membrane interiors if palmitoylated endodomain cysteines were nearby to presumably keep the spans from adopting a perpendicular orientation relative to the membrane. If this concept applies to the S proteins, then extracellular extension from the membrane bilayer might be progressively more oblique with increasing endodomain palmitoylation, and in turn, the degree to which HR2 regions remain separated and poised for the membrane fusion reaction would relate to the extent of endodomain palmitoylation.

One final and obvious point about our study is that the workings of viral fusion proteins can only be partially understood by analyzing the structure and function of soluble protein ectodomains. The way that viral fusion proteins are embedded into virion and infected cell membranes is crucial to our understanding. For the coronaviruses, extensive palmitoylation of fusion protein endodomains may set up a metastable membrane embedment that is both preferentially selected for assembly into virions and set up for rapid membrane fusion-related refolding.

Acknowledgments—We thank Heidi Olivares for expert technical assistance. We are grateful to Fumihiro Taguchi (National Institute of Infectious Diseases, Tokyo, Japan) and John Fleming (University of Wisconsin) for antiviral antibodies used in this study. We also thank Paul Masters (Wadsworth Center, Albany, NY) for providing the reagents necessary to construct recombinant MHVs. Finally, we thank Berend Jan Bosch (Utrecht University, Netherlands) for important and insightful discussions that were relevant to this study.

REFERENCES

1. Harrison, S. C. (2008) *Nat. Struct. Mol. Biol.* **15,** 690–698
2. White, J. M., Delos, S. E., Brecher, M., and Schornberg, K. (2008) *Crit. Rev. Biochem. Mol. Biol.* **43,** 189–219
3. Mothes, W., Boerger, A. L., Narayan, S., Cunningham, J. M., and Young, J. A. (2000) *Cell* **103,** 679–689
4. Simmons, G., Reeves, J. D., Rennekamp, A. J., Amberg, S. M., Piefer, A. J., and Bates, P. (2004) *Proc. Natl. Acad. Sci. U.S.A.* **101,** 4240–4245
5. Chandran, K., Sullivan, N. J., Felbor, U., Whelan, S. P., and Cunningham, J. M. (2005) *Science* **308,** 1643–1645
6. Chernomordik, L. V., and Kozlov, M. M. (2008) *Nat. Struct. Mol. Biol.* **15,** 675–683
7. Melikyan, G. B., Markosyan, R. M., Hemmati, H., Delmedico, M. K., Lambert, D. M., and Cohen, F. S. (2000) *J. Cell Biol.* **151,** 413–423
8. Skehel, J. J., and Wiley, D. C. (2000) *Annu. Rev. Biochem.* **69,** 531–569
9. Langosch, D., Hofmann, M., and Ungermann, C. (2007) *Cell Mol. Life Sci.* **64,** 850–864
10. Abrahamyan, L. G., Mkrtchyan, S. R., Binley, J., Lu, M., Melikyan, G. B., and Cohen, F. S. (2005) *J. Virol.* **79,** 106–115
11. Cathomen, T., Naim, H. Y., and Cattaneo, R. (1998) *J. Virol.* **72,** 1224–1234
12. Sakai, T., Ohuchi, R., and Ohuchi, M. (2002) *J. Virol.* **76,** 4603–4611
13. Kemble, G. W., Danieli, T., and White, J. M. (1994) *Cell* **76,** 383–391
14. Green, N., Shinnick, T. M., Witte, O., Ponticelli, A., Sutcliffe, J. G., and Lerner, R. A. (1981) *Proc. Natl. Acad. Sci. U.S.A.* **78,** 6023–6027
15. Yang, C., and Compans, R. W. (1996) *J. Virol.* **70,** 248–254
16. Wyss, S., Dimitrov, A. S., Baribaud, F., Edwards, T. G., Blumenthal, R., and Hoxie, J. A. (2005) *J. Virol.* **79,** 12231–12241
17. Yin, H. S., Paterson, R. G., Wen, X., Lamb, R. A., and Jardetzky, T. S. (2005) *Proc. Natl. Acad. Sci. U.S.A.* **102,** 9288–9293
18. Markosyan, R. M., Cohen, F. S., and Melikyan, G. B. (2003) *Mol. Biol. Cell* **14,** 926–938
19. Chernomordik, L. V., and Kozlov, M. M. (2003) *Annu. Rev. Biochem.* **72,** 175–207
20. Rota, P. A., Oberste, M. S., Monroe, S. S., Nix, W. A., Campagnoli, R., Icenogle, J. P., Peñaranda, S., Bankamp, B., Maher, K., Chen, M. H., Tong, S., Tamin, A., Lowe, L., Frace, M., DeRisi, J. L., Chen, Q., Wang, D., Erdman, D. D., Peret, T. C., Burns, C., Ksiazek, T. G., Rollin, P. E., Sanchez, A., Liffick, S., Holloway, B., Limor, J., McCaustland, K., Olsen-Rasmussen, M., Fouchier, R., Günther, S., Osterhaus, A. D., Drosten, C., Pallansch, M. A., Anderson, L. J., and Bellini, W. J. (2003) *Science* **300,** 1394–1399
21. Delmas, B., and Laude, H. (1990) *J. Virol.* **64,** 5367–5375
22. Bosch, B. J., van der Zee, R., de Haan, C. A., and Rottier, P. J. (2003) *J. Virol.* **77,** 8801–8811
23. Madu, I. G., Roth, S. L., Belouzard, S., and Whittaker, G. R. (2009) *J. Virol.* **83,** 7411–7421
24. de Groot, R. J., Luytjes, W., Horzinek, M. C., van der Zeijst, B. A., Spaan, W. J., and Lenstra, J. A. (1987) *J. Mol. Biol.* **196,** 963–966
25. Tripet, B., Howard, M. W., Jobling, M., Holmes, R. K., Holmes, K. V., and Hodges, R. S. (2004) *J. Biol. Chem.* **279,** 20836–20849
26. Supekar, V. M., Bruckmann, C., Ingallinella, P., Bianchi, E., Pessi, A., and Carfí, A. (2004) *Proc. Natl. Acad. Sci. U.S.A.* **101,** 17958–17963
27. Xu, Y., Liu, Y., Lou, Z., Qin, L., Li, X., Bai, Z., Pang, H., Tien, P., Gao, G. F., and Rao, Z. (2004) *J. Biol. Chem.* **279,** 30514–30522
28. Bos, E. C., Heijnen, L., Luytjes, W., and Spaan, W. J. (1995) *Virology* **214,** 453–463
29. Thorp, E. B., Boscarino, J. A., Logan, H. L., Goletz, J. T., and Gallagher, T. M. (2006) *J. Virol.* **80,** 1280–1289
30. Petit, C. M., Chouljenko, V. N., Iyer, A., Colgrove, R., Farzan, M., Knipe, D. M., and Kousoulas, K. G. (2007) *Virology* **360,** 264–274
31. Chang, K. W., Sheng, Y., and Gombold, J. L. (2000) *Virology* **269,** 212–224
32. Veit, M., Kretzschmar, E., Kuroda, K., Garten, W., Schmidt, M. F., Klenk, H. D., and Rott, R. (1991) *J. Virol.* **65,** 2491–2500
33. Yang, C., Spies, C. P., and Compans, R. W. (1995) *Proc. Natl. Acad. Sci. U.S.A.* **92,** 9871–9875
34. Chang, K. W., and Gombold, J. L. (2001) *Adv. Exp. Med. Biol.* **494,** 205–211
35. Sturman, L. S., and Takemoto, K. K. (1972) *Infect. Immun.* **6,** 501–507
36. Pedersen, N. C., Boyle, J. F., Floyd, K., Fudge, A., and Barker, J. (1981) *Am. J. Vet. Res.* **42,** 368–377
37. Rao, P. V., and Gallagher, T. M. (1998) *J. Virol.* **72,** 3278–3288
38. Masters, P. S., and Rottier, P. J. (2005) *Curr. Top. Microbiol. Immunol.* **287,** 133–159
39. Kuo, L., Godeke, G. J., Raamsman, M. J., Masters, P. S., and Rottier, P. J. (2000) *J. Virol.* **74,** 1393–1406
40. Niwa, H., Yamamura, K., and Miyazaki, J. (1991) *Gene* **108,** 193–199
41. Boscarino, J. A., Logan, H. L., Lacny, J. J., and Gallagher, T. M. (2008) *J. Virol.* **82,** 2989–2999
42. Wigler, M., Pellicer, A., Silverstein, S., and Axel, R. (1978) *Cell* **14,** 725–731
43. Graham, F. L., and van der Eb, A. J. (1973) *Virology* **52,** 456–467
44. Gallagher, T. M. (1997) *J. Virol.* **71,** 3129–3137
45. Grosse, B., and Siddell, S. G. (1994) *Virology* **202,** 814–824
46. Fleming, J. O., Stohlman, S. A., Harmon, R. C., Lai, M. M., Frelinger, J. A., and Weiner, L. P. (1983) *Virology* **131,** 296–307
47. Matsuyama, S., and Taguchi, F. (2002) *J. Virol.* **76,** 11819–11826
48. McShane, M. P., and Longnecker, R. (2005) *Methods Mol. Biol.* **292,** 187–196
49. Aoki, Y., Aizaki, H., Shimoike, T., Tani, H., Ishii, K., Saito, I., Matsuura, Y., and Miyamura, T. (1998) *Virology* **250,** 140–150
50. de Haan, C. A., van Genne, L., Stoop, J. N., Volders, H., and Rottier, P. J. (2003) *J. Virol.* **77,** 11312–11323
51. Masters, P. S., Kuo, L., Ye, R., Hurst, K. R., Koetzner, C. A., and Hsue, B. (2006) *Adv. Exp. Med. Biol.* **581,** 163–173
52. de Haan, C. A., Smeets, M., Vernooij, F., Vennema, H., and Rottier, P. J. (1999) *J. Virol.* **73,** 7441–7452
53. Opstelten, D. J., Raamsman, M. J., Wolfs, K., Horzinek, M. C., and Rottier, P. J. (1995) *J. Cell Biol.* **131,** 339–349
54. Chan, D. C., and Kim, P. S. (1998) *Cell* **93,** 681–684
55. Furuta, R. A., Wild, C. T., Weng, Y., and Weiss, C. D. (1998) *Nat. Struct.*

Biol. **5,** 276–279
56. Bosch, B. J., Martina, B. E., Van Der Zee, R., Lepault, J., Haijema, B. J., Versluis, C., Heck, A. J., De Groot, R., Osterhaus, A. D., and Rottier, P. J. (2004) *Proc. Natl. Acad. Sci. U.S.A.* **101,** 8455–8460
57. Zelus, B. D., Schickli, J. H., Blau, D. M., Weiss, S. R., and Holmes, K. V. (2003) *J. Virol.* **77,** 830–840
58. Krueger, D. K., Kelly, S. M., Lewicki, D. N., Ruffolo, R., and Gallagher, T. M. (2001) *J. Virol.* **75,** 2792–2802
59. Yan, Z., Tripet, B., and Hodges, R. S. (2006) *J. Struct. Biol.* **155,** 162–175
60. Shang, L., Yue, L., and Hunter, E. (2008) *J. Virol.* **82,** 5417–5428
61. Helseth, E., Olshevsky, U., Gabuzda, D., Ardman, B., Haseltine, W., and Sodroski, J. (1990) *J. Virol.* **64,** 6314–6318
62. Melikyan, G. B., Lin, S., Roth, M. G., and Cohen, F. S. (1999) *Mol. Biol. Cell* **10,** 1821–1836
63. Broer, R., Boson, B., Spaan, W., Cosset, F. L., and Corver, J. (2006) *J. Virol.* **80,** 1302–1310
64. Bissonnette, M. L., Donald, J. E., DeGrado, W. F., Jardetzky, T. S., and Lamb, R. A. (2009) *J. Mol. Biol.* **386,** 14–36
65. Yang, L., and Huang, H. W. (2002) *Science* **297,** 1877–1879
66. Cohen, F. S., and Melikyan, G. B. (2004) *J. Membr. Biol.* **199,** 1–14
67. Bosch, B. J., de Haan, C. A., Smits, S. L., and Rottier, P. J. (2005) *Virology* **334,** 306–318
68. Ye, R., Montalto-Morrison, C., and Masters, P. S. (2004) *J. Virol.* **78,** 9904–9917
69. Rousso, I., Mixon, M. B., Chen, B. K., and Kim, P. S. (2000) *Proc. Natl. Acad. Sci. U.S.A.* **97,** 13523–13525
70. Chen, B. J., Takeda, M., and Lamb, R. A. (2005) *J. Virol.* **79,** 13673–13684
71. Ono, A., and Freed, E. O. (2001) *Proc. Natl. Acad. Sci. U.S.A.* **98,** 13925–13930
72. Zhang, J., Pekosz, A., and Lamb, R. A. (2000) *J. Virol.* **74,** 4634–4644
73. Melkonian, K. A., Ostermeyer, A. G., Chen, J. Z., Roth, M. G., and Brown, D. A. (1999) *J. Biol. Chem.* **274,** 3910–3917
74. Tooze, J., Tooze, S., and Warren, G. (1984) *Eur. J. Cell Biol.* **33,** 281–293
75. Krijnse-Locker, J., Ericsson, M., Rottier, P. J., and Griffiths, G. (1994) *J. Cell Biol.* **124,** 55–70
76. van Meer, G., Voelker, D. R., and Feigenson, G. W. (2008) *Nat. Rev. Mol. Cell Biol.* **9,** 112–124
77. Nguyen, D. H., and Hildreth, J. E. (2000) *J. Virol.* **74,** 3264–3272
78. Qiu, Z., Hingley, S. T., Simmons, G., Yu, C., Das Sarma, J., Bates, P., and Weiss, S. R. (2006) *J. Virol.* **80,** 5768–5776
79. McReynolds, S., Jiang, S., Guo, Y., Celigoy, J., Schar, C., Rong, L., and Caffrey, M. (2008) *Biochemistry* **47,** 6802–6808
80. Zhu, P., Liu, J., Bess, J., Jr., Chertova, E., Lifson, J. D., Grisé, H., Ofek, G. A., Taylor, K. A., and Roux, K. H. (2006) *Nature* **441,** 847–852
81. Zhou, T., Xu, L., Dey, B., Hessell, A. J., Van Ryk, D., Xiang, S. H., Yang, X., Zhang, M. Y., Zwick, M. B., Arthos, J., Burton, D. R., Dimitrov, D. S., Sodroski, J., Wyatt, R., Nabel, G. J., and Kwong, P. D. (2007) *Nature* **445,** 732–737
82. Abrami, L., Kunz, B., Iacovache, I., and van der Goot, F. G. (2008) *Proc. Natl. Acad. Sci. U.S.A.* **105,** 5384–5389